

A fast and accurate numerical method for the symmetric Lévy processes based on the Fourier transform and sinc-Gauss sampling formula

KEN'ICHIRO TANAKA[†]

Future University Hakodate, 116-2, Kamedanakano-cho, Hakodate, Hokkaido, Japan

[1 August 2014]

In this paper, we propose a fast and accurate numerical method based on Fourier transform to solve Kolmogorov forward equations of symmetric scalar Lévy processes. The method is based on the accurate numerical formulas for Fourier transform proposed by Ooura. These formulas are combined with nonuniform fast Fourier transform (FFT) and fractional FFT to speed up the numerical computations. Moreover, we propose a formula for numerical indefinite integration on equispaced grids as a component of the method. The proposed integration formula is based on the sinc-Gauss sampling formula, which is a function approximation formula. This integration formula is also combined with the FFT. Therefore, all steps of the proposed method are executed using the FFT and its variants. The proposed method allows us to be free from some special treatments for a non-smooth initial condition and numerical time integration. The numerical solutions obtained by the proposed method appeared to be exponentially convergent on the interval if the corresponding exact solutions do not have sharp cusps. Furthermore, the real computational times are approximately consistent with the theoretical estimates.

Keywords: Lévy process; Kolmogorov forward equation; nonuniform FFT; fractional FFT; sinc-Gauss sampling formula.

1. Introduction

In this paper, we propose a fast and accurate numerical method based on the Fourier transform to solve the Kolmogorov forward equations of the symmetric scalar Lévy processes. To propose the method, we use Ooura's accurate numerical formulas for the Fourier transform (Ooura, 2001, 2005), and propose a numerical indefinite integration formula based on the sinc-Gauss sampling formula (Tanaka *et al.*, 2008) to compute the integrals with respect to the Lévy measures in the equation. Furthermore, we combine the fast Fourier transform (FFT) with these formulas to speed up the numerical computations.

A Lévy process $\{X_t\}_{t \geq 0}$ is essentially a stochastic process with stationary and independent increments (Applebaum, 2009), which is used to describe uncertain phenomena in various fields. Let us consider a brief non-rigorous review of the scalar Lévy process $\{X_t\}_{t \geq 0}$. The Lévy-Khintchine theorem characterizes X_t by reals $b \in \mathbf{R}$, $a \geq 0$, and a Borel measure ν on $\mathbf{R} \setminus \{0\}$ as

$$\mathbb{E}[e^{iuX_t}] = e^{t\psi(u)}, \quad (1.1)$$

where ψ is the characteristic exponent of X_1 defined by

$$\psi(u) = ibu - \frac{1}{2}a^2u^2 + \int_{\mathbf{R} \setminus \{0\}} \left(e^{iuy} - 1 - iuy\mathbf{1}_{|y| \leq 1}(y) \right) \nu(dy). \quad (1.2)$$

[†]Email: ketanaka@fun.ac.jp

Here, we assume that the measure ν satisfies

$$\int_{\mathbf{R} \setminus \{0\}} \min \{y^2, 1\} \nu(dy) < \infty. \quad (1.3)$$

Then, ν is called the Lévy measure. An operator semigroup $\{T_t\}_{t \geq 0}$ is associated with $\{X_t\}_{t \geq 0}$, namely $(T_t f)(x) = E[f(X_t) | X_0 = x]$, where f is a bounded continuous function on \mathbf{R} . The infinitesimal generator $A = \frac{d}{dt}(T_t f) |_{t=0}$ takes the form

$$(Af)(x) = b f'(x) + a f''(x) + \int_{\mathbf{R} \setminus \{0\}} [f(x+y) - f(x) - y \mathbf{1}_{|y| \leq 1}(y) f'(x)] \nu(dy). \quad (1.4)$$

Then, the function $u(x, t) = (T_t f)(x)$ is the solution of the partial integro-differential equation (PIDE)

$$\frac{\partial u}{\partial t}(x, t) = A u(x, t) \quad (x \in \mathbf{R}, t \geq 0) \quad (1.5)$$

with initial condition $u(x, 0) = f(x)$. Assuming that there exist the transition probability measure $p(x_0, 0; x, t)$ of X_t with appropriate continuity and differentiability for each $t \geq 0$ and the adjoint operator A^\dagger of A , we have

$$\frac{\partial p}{\partial t}(x_0, 0; x, t) = A^\dagger p(x_0, 0; x, t) \quad (x \in \mathbf{R}, t \geq 0) \quad (1.6)$$

with initial condition $p(x_0, 0; x, 0) = \delta(x - x_0)$, where δ is the Dirac delta function. Equation (1.6) is the Kolmogorov forward equation, which is also known as the Fokker-Planck equation. Furthermore, the equation

$$\frac{\partial v}{\partial s}(x, t - s) = -A v(x, t - s) \quad (x \in \mathbf{R}, s \leq t) \quad (1.7)$$

with initial condition $v(x, t) = f(x)$ is known as the Kolmogorov backward equation.

In various fields such as physics, chemistry, biology, engineering, and economics, the Kolmogorov forward equations including fractional derivatives are often considered to describe some unusual diffusion such as anomalous diffusion. For example, see Gardiner (2009); Kozubowski *et al.* (2006); Lenzi *et al.* (2003); Sabatier *et al.* (2007); Yan (2013) and the references therein. Such equations are related to α -stable processes belonging to the Lévy processes. In finance, some Lévy processes are used to describe the prices of risk assets. Then, the Kolmogorov backward equations for these processes are considered as one of the useful methods for option pricing. See Cont & Voltchkova (2005); Garreau & Kopriva (2013); Lee *et al.* (2012) and the references therein.

In the fields mentioned above, many numerical methods for these Kolmogorov equations are studied. Popular examples of such methods are finite difference methods (Gao *et al.*, 2013; Huang & Oberman, 2013; Li *et al.*, 2012; Meerschaert, 2004), finite element methods (Zhao & Lib, 2012), spectral methods (Bueno-Orovio *et al.*, 2014; Huang *et al.*, 2014), and other methods (Yan, 2013) for the forward equations describing anomalous diffusion etc. Further, such methods have been proposed for the backward equations in finance (Duquesne *et al.*, 2010; Garreau & Kopriva, 2013; Kwok *et al.*, 2012; Lee *et al.*, 2012). In many of these methods, first, a time-evolution system of ordinary differential equations is derived from the given PIDE by the discretization of the spatial variable with finite differences, finite elements, polynomial expansions, etc., and some quadrature formulas. Then, the system is numerically

solved using some numerical time integration methods such as second-order finite difference methods. In addition, in the case where the closed form of the characteristic function of the Lévy process can be obtained, methods based on the Fourier series or the Fourier transform are used in option pricing (Carr & Madan, 1999; Chourdakis, 2005; Fang & Oosterlee, 2008; Kwok *et al.*, 2012).

In this paper, we propose a method based on the Fourier transform for equation (1.6) for broader classes of the Lévy measure ν for which the closed form of the corresponding characteristic function may not be available. For simplicity, we consider the case $b = a = 0$ in (1.4) and measure ν has the form

$$\nu(dy) = \frac{1}{|y|^\gamma} \mu(|y|) dy, \quad (1.8)$$

where $\gamma = 1$ or $\gamma = 2$ and $\mu \in L^1(0, \infty)$. Then, the corresponding Lévy process becomes symmetric. As examples of the Lévy process with such measure, we can give the variance gamma (VG) process (Applebaum, 2009), also known as the symmetric Laplace motion (Kozubowski *et al.*, 2006), with $\gamma = 1$ and $\mu(y) = e^{-y}$, and the normal inverse Gaussian (NIG) process (Applebaum, 2009) with $\gamma = 2$ and $\mu(y) = yK_1(y)/\pi$, where K_1 is the modified Bessel function of the second kind. Then, applying (1.8) to the operator A in (1.4) and taking its adjoint, we have a special form of equation (1.6) as

$$\frac{\partial p}{\partial t}(x, t) = E_\gamma^+ p(x, t) + E_\gamma^- p(x, t) \quad (x \in \mathbf{R}, t \geq 0), \quad (1.9)$$

where $p(x_0, 0; x, t)$ is denoted by $p(x, t)$ for conciseness, and

$$E_\gamma^\pm q(x) = \int_0^\infty \frac{q(x \pm y) - q(x)}{y^\gamma} \mu(y) dy. \quad (1.10)$$

Note that the third term of the integrand in (1.4) vanishes because of the symmetry of ν . Furthermore, we assume that $x_0 = 0$ for simplicity and $p(x, t) \rightarrow 0$ as $|x| \rightarrow 0$ for any $t \geq 0$ so that

$$\int_{-\infty}^\infty p(x, t) dx = 1 \quad (1.11)$$

for any $t \geq 0$. Therefore, we consider equation (1.9) with initial condition $p(x, 0) = \delta(x)$ and auxiliary condition (1.11) in the rest of this paper.

There are two main objectives of the method proposed in this paper. The first is to show that a fast and accurate Fourier-based method can be realized for equation (1.9) including a (seemingly) singular integral in (1.10). Using the Fourier transform, we do not need specific requirements for the non-smooth initial condition $p(x, 0) = \delta(x)$, whereas some of the existing methods with time integration cited above need a priori artificial approximation of the solution $p(x, t)$ for a small time t . In addition, since equation (1.9) is linear and contains only constant coefficients, which is also the case for the general A in (1.4), the Fourier-based method does not need numerical time integration. Therefore, we can compute approximate solutions of $p(x, t)$ for any t with the same computational cost, and errors of numerical time integration do not occur. The second objective of the proposed method is to present new applications of Ooura's methods (Ooura, 2001, 2005) for the Fourier transforms to obtain the solution of PIDEs. The high accuracy of the proposed method is due to the very fast convergence of Ooura's methods, and speeding up of computations by Ooura's methods is realized by combining them with the nonuniform FFT (Dutt & Rokhlin, 1993, 1995; Greengard & Lee, 2004; Potts *et al.*, 2001; Steidl, 1998) or the fractional FFT (Bailey & Swarztrauber, 1991; Chourdakis, 2005; Tanaka, 2014a). In addition,

in order to treat a (seemingly) singular integral in (1.10), we propose an indefinite integration formula using the sinc-Gauss sampling formula (Tanaka *et al.*, 2008), which is also accurate and combined with the FFT. Thus, as shown precisely in Sections 2 and 3, all steps of the proposed method are executed by the FFT and its variants.

The remainder of this paper is organized as follows. Section 2 contains the outline of the proposed method, which consists of three steps. Section 3 details the three steps. Section 4 shows the actual performance of the proposed method through numerical examples, and Section 5 concludes this paper.

2. Outline of the proposed method

In order to obtain a fast and accurate numerical method to solve (1.9), we considered a method based on the Fourier transform for using the FFT. First, we derive the formula for the solution of (1.9) using the Fourier transform

$$[\mathcal{F}f](\omega) = \int_{-\infty}^{\infty} f(x) e^{-i\omega x} dx. \quad (2.1)$$

Taking the Fourier transform for both sides of (1.9) with respect to the spatial variable x , we have

$$\frac{\partial [\mathcal{F}p]}{\partial t}(\omega, t) = [\mathcal{G}_\gamma \mu](\omega) [\mathcal{F}p](\omega, t), \quad (2.2)$$

where

$$[\mathcal{G}_\gamma \mu](\omega) = \int_0^\infty \frac{e^{-i\omega y} - 1}{y^\gamma} \mu(y) dy + \int_0^\infty \frac{e^{+i\omega y} - 1}{y^\gamma} \mu(y) dy. \quad (2.3)$$

For $\gamma = 1$, noting that $\mu \in L^1(0, \infty)$, we have

$$\begin{aligned} \int_0^\infty \frac{e^{\mp i\omega y} - 1}{y} \mu(y) dy &= \int_0^\infty \left(\mp i \int_0^\omega e^{\mp i\zeta y} d\zeta \right) \mu(y) dy \\ &= \mp i \int_0^\omega \left(\int_0^\infty \mu(y) e^{\mp i\zeta y} dy \right) d\zeta, \end{aligned} \quad (2.4)$$

and therefore,

$$[\mathcal{G}_1 \mu](\omega) = 2 \operatorname{Im} \int_0^\omega \left(\int_0^\infty \mu(y) e^{-i\zeta y} dy \right) d\zeta. \quad (2.5)$$

For $\gamma = 2$, noting that

$$\begin{aligned} &\int_0^\infty \frac{e^{-i\omega y} - 1}{y^2} \mu(y) dy + \int_0^\infty \frac{e^{+i\omega y} - 1}{y^2} \mu(y) dy \\ &= \int_0^\infty \frac{e^{-i\omega y} - 1 + i\omega y}{y^2} \mu(y) dy + \int_0^\infty \frac{e^{+i\omega y} - 1 - i\omega y}{y^2} \mu(y) dy \end{aligned}$$

and $\mu \in L^1(0, \infty)$, we have

$$\int_0^\infty \frac{e^{\mp i\omega y} - 1 \pm i\omega y}{y^2} \mu(y) dy = \int_0^\infty \left(- \int_0^\omega \int_0^\eta e^{\mp i\zeta y} d\zeta d\eta \right) \mu(y) dy$$

$$= - \int_0^\omega \int_0^\eta \left(\int_0^\infty \mu(y) e^{\mp i \zeta y} dy \right) d\zeta d\eta. \quad (2.6)$$

Therefore, we have

$$[\mathcal{G}_2 \mu](\omega) = -2 \operatorname{Re} \int_0^\omega \int_0^\eta \left(\int_0^\infty \mu(y) e^{-i \zeta y} dy \right) d\zeta d\eta. \quad (2.7)$$

Using expression (2.5) or (2.7), we can derive the form of the solution $p(x, t)$ from (2.2) as

$$p(x, t) = \mathcal{F}^{-1} \left[\exp(t [\mathcal{G}_\gamma \mu]) \right] (x) = \frac{1}{2\pi} \int_{-\infty}^\infty \exp(t [\mathcal{G}_\gamma \mu](\omega)) e^{ix\omega} d\omega. \quad (2.8)$$

Then, we can consider the following numerical method to obtain an approximation of the solution (2.8). Let $N > 0$, $\tilde{h} > 0$, and $t > 0$ be an integer, a grid spacing, and a time, respectively. Suppose that we need to compute approximate values of $p(x, t)$ for $x = n\tilde{h}$ ($n = -N + 1, \dots, N$).

Step 1 Computation of the Fourier transform

$$\int_0^\infty \mu(y) e^{-i \zeta y} dy \quad (2.9)$$

in (2.5) or (2.7). Choose a grid spacing $\tilde{h} > 0$ and integers $M_-, M_+, N_\gamma > 0$. Then, use *the double exponential (DE) formula for the Fourier transforms* (Ooura, 2005) with sampling points $y = y_j$ ($j = -M_-, \dots, M_+ - 1$) and *the nonuniform FFT* (Dutt & Rokhlin, 1993, 1995; Greengard & Lee, 2004; Potts *et al.*, 2001; Steidl, 1998) to obtain approximate values of (2.9) for $\zeta = k\tilde{h}$ ($k = -N_\gamma + 1, \dots, N_\gamma$). The definitions of $\tilde{h}, M_-, M_+, N_\gamma$, and y_j are presented in Sections 3.1 and 3.2.

Step 2 Computation of the indefinite integral of (2.9) in (2.5) or (2.7). Use the computed values in Step 1 and *an indefinite integration by the sinc-Gauss sampling formula* proposed in Section 3.2 to obtain approximate values of $[\mathcal{G}_\gamma \mu](\omega)$ for $\omega = \ell\tilde{h}$ ($\ell = -N_\gamma/2^\gamma + 1, \dots, N_\gamma/2^\gamma$), where we suppose that N_γ can be divided by 2^γ . Note that the approximate values on the equispaced grid are obtained from the approximate values of the integrand on the same grid. The definition of N_γ is presented in Section 3.2.

Step 3 Computation of the inverse Fourier transform (2.8). Use the computed values in Step 2, *the formula for the Fourier transform with continuous Euler transform* (Ooura, 2001), and *the fractional FFT* (Bailey & Swartztrauber, 1991; Chourdakis, 2005; Tanaka, 2014a) to obtain the approximate values of the solution $p(x, t)$ for $x = n\tilde{h}$ ($n = -N + 1, \dots, N$).

In summary, the proposed method is illustrated by the diagram below. The details of the three steps are shown in Section 3.

The Kolmogorov forward equation (1.9) for the Lévy process with measure given by (1.8)

(Step 1)
DE formula for FT
+ nonuniform FFT

Approximate values of (2.9):

$$\int_0^\infty \mu(y) e^{-i\zeta y} dy$$

(Step 2)
↓ sinc-Gauss indefinite integration

Approximate values of the solution (2.8):

$$p(x, t) = \mathcal{F}^{-1} [\exp(t [\mathcal{G}_\gamma \mu])] (x)$$

(Step 3)
Formula with continuous
Euler transform for FT
+ fractional FFT

Approximate values of $[\mathcal{G}_\gamma \mu](\omega)$ in (2.5) or (2.7).

3. Proposed method

3.1 Step 1: Computation of the Fourier transform (2.9) in (2.5) or (2.7)

The DE formula for the Fourier transforms and the nonuniform FFT for the Fourier transform (2.9) are described in Sections 3.1.1 and 3.1.2, respectively. The contribution of this paper is speeding up the computation through the use of the DE formula by combining it with nonuniform FFT.

3.1.1 DE formula for the Fourier transforms by Ooura. We begin with the review of the DE formula for the Fourier transforms (2.9) proposed by Ooura (2005). Let ζ_0 and h be positive constants and let the function $\varphi : \mathbf{R} \rightarrow (0, \infty)$ be defined by

$$\varphi(t) = \frac{t}{1 - \exp(-2t - \alpha(1 - e^{-t}) - \beta(e^t - 1))}, \quad (3.1)$$

where $\beta = 0.25$ and

$$\alpha = \frac{\beta}{\sqrt{1 + \log(1 + \pi/(\zeta_0 h))}/(4\zeta_0 h)}. \quad (3.2)$$

Then, the following formula approximates the integral (2.9) for $\zeta \in (\delta_1, 2\zeta_0 - \delta_2)$ for some $\delta_1, \delta_2 \geq 0$:

$$\begin{aligned} & \int_0^\infty \mu(y) e^{-i\zeta y} dy \\ & \approx -\frac{2\pi i}{\zeta_0} \sum_{j=-M_-}^{M_+-1} \left[\mu\left(\frac{\pi}{\zeta_0 h} \varphi(jh)\right) \sin\left(\frac{\pi}{2h} \hat{\varphi}(jh)\right) \varphi'(jh) \exp\left(\frac{\pi i}{2h} \hat{\varphi}(jh)\right) \right] \exp\left(-\frac{\pi i \zeta}{\zeta_0 h} \varphi(jh)\right). \end{aligned} \quad (3.3)$$

where $\hat{\varphi}(t) = \varphi(t) - t$. The integers M_- and M_+ are determined in an appropriate manner. Formula (3.3) is the DE formula for the Fourier transforms, which is derived as follows. First, applying the variable transformation $y = (\pi/(\zeta_0 h)) \varphi(t)$ to integral (2.9), we have

$$\int_0^\infty \mu(y) e^{-i\zeta y} dy = \int_{-\infty}^\infty \mu(P\varphi(t)) \exp(-i\zeta P\varphi(t)) P\varphi'(t) dt, \quad (3.4)$$

where $P = \pi/(\zeta_0 h)$. Let $\mathcal{M}(\zeta)$ denote expression (3.4). Next, from $\mathcal{M}(\zeta)$ subtract

$$\mathcal{N}(\zeta) = \int_{-\infty}^\infty \mu(P\varphi(t)) \exp(-i\zeta P\varphi(t) + i\zeta_0 P\hat{\varphi}(t)) P\varphi'(t) dt, \quad (3.5)$$

which is very small for $\zeta \in (\delta_1, 2\zeta_0 - \delta_2)$ and a large P . Then, discretizing

$$\mathcal{M}(\zeta) - \mathcal{N}(\zeta) = -\frac{2\pi i}{\zeta_0 h} \int_{-\infty}^{\infty} \mu \left(\frac{\pi}{\zeta_0 h} \varphi(t) \right) \sin \left(\frac{\pi}{2h} \hat{\varphi}(t) \right) \varphi'(t) \exp \left(-\frac{\pi i \zeta}{\zeta_0 h} \varphi(t) + \frac{\pi i}{2h} \hat{\varphi}(t) \right) dt \quad (3.6)$$

by the mid-point rule with grid spacing h , we have (3.3). Since $\hat{\varphi}(t) \rightarrow 0$ as $t \rightarrow -\infty$ and $\varphi'(t) \rightarrow 0$ as $t \rightarrow +\infty$, the factor $[\sin(\frac{\pi}{2h} \hat{\varphi}(t)) \varphi'(t)]$ in (3.6) converges rapidly (“double exponentially”) to 0 as $t \rightarrow \pm\infty$. Therefore, the discretization of (3.6) by the mid-point rule can yield accurate approximation (3.3) for some h independent of ζ , and sufficiently large M_+ and M_- . In Ooura (2005), the error of approximation (3.3) is bounded by $c'_0 e^{-c_0/h} + c'_1 e^{-c_1 \zeta/h} + c'_2 e^{-c_2(2\zeta_0 - \zeta)/h}$ for some c_i, c'_i depending on μ , and it is illustrated by some numerical examples. A theoretically rigorous analysis for the error, however, is not described in Ooura (2005).

Then, noting that

$$\int_0^{\infty} \mu(y) e^{-i(-\zeta)y} dy = \overline{\int_0^{\infty} \mu(y) e^{-i\zeta y} dy}, \quad (3.7)$$

we can achieve Step 1 by computing the values of (3.3) for $\zeta = k\tilde{h}$ ($k = 0, \dots, N_\gamma$) and taking their complex conjugates for $\zeta = -k\tilde{h}$ ($k = 0, \dots, N_\gamma$). In computing the values of (3.3), we need to choose ζ_0 so that $k\tilde{h} \in (\delta_1, 2\zeta_0 - \delta_2)$ for $k = 0, \dots, N_\gamma$. The possible values of the nonnegative reals δ_1 and δ_2 , however, are not theoretically estimated. According to some numerical examples including those in Ooura (2005), when ζ_0 is small, δ_1 can be taken as $\delta_1 = 0$ and δ_2 can be small. As ζ_0 becomes large, unfortunately, δ_1 and δ_2 need to be large. These facts are illustrated by Figure 1. Therefore, if we let ζ_0 be a single value near to $N_\gamma \tilde{h}/2$ when $N_\gamma \tilde{h}$ is large, we cannot have accurate approximations of (2.9) for $\zeta = k\tilde{h}$ for k 's near to 0 or N_γ . Then, we use

$$\zeta_0 = N_\gamma \tilde{h}/15 \quad \text{to compute (2.9) for } \zeta = 0, \tilde{h}, \dots, \lfloor N_\gamma/8 \rfloor \tilde{h}, \quad (3.8)$$

$$\zeta_0 = N_\gamma \tilde{h}/1.8 \quad \text{to compute (2.9) for } \zeta = (\lfloor N_\gamma/8 \rfloor + 1)\tilde{h}, \dots, N_\gamma \tilde{h}. \quad (3.9)$$

Figure 1 also illustrates these settings, which are experientially determined and not based on theoretical criteria.

Note that the naive computation of (3.3) for (3.8) and (3.9) requires $O(N_\gamma^2)$ operations if $M_+ + M_- \propto N_\gamma$. Then, what remains in Step 1 is to speed up the numerical computation. Thus, we use the technique of the nonuniform FFT explained in Section 3.1.2 below.

3.1.2 Nonuniform FFT. Let the sum in (3.3) for $\zeta = k\tilde{h}$ be rewritten as

$$\hat{\mu}_k = \sum_{j=-M_-}^{M_+-1} \Phi[\mu]_j \exp(-i k \tilde{h} y_j), \quad (3.10)$$

where

$$\Phi[\mu]_j = -\frac{2\pi i}{\zeta_0} \left[\mu \left(\frac{\pi}{\zeta_0 h} \varphi(jh) \right) \sin \left(\frac{\pi}{2h} \hat{\varphi}(jh) \right) \varphi'(jh) \exp \left(\frac{\pi i}{2h} \hat{\varphi}(jh) \right) \right], \quad (3.11)$$

$$y_j = \frac{\pi}{\zeta_0 h} \varphi(jh). \quad (3.12)$$

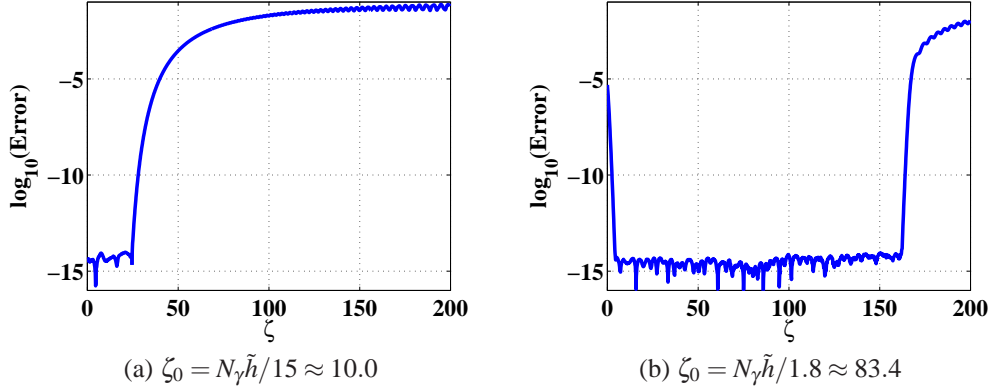


FIG. 1. Errors of the approximate values (3.3) for the Fourier transform (2.9) of $\mu(y) = e^{-y}$. The parameters M_- , M_+ , and h in (3.3) are defined by $M_- = M_+ = 2^{10}$, and $h = \log(10^3 M)/M \approx 0.007$, where $M = M_- + M_+ = 2^{11}$. In addition, two cases for ζ_0 in (3.3) are considered: (a) $\zeta_0 = N_\gamma \tilde{h}/15 \approx 10.0$, and (b) $\zeta_0 = N_\gamma \tilde{h}/1.8 \approx 83.4$, where $N_\gamma = M/2 = 2^9$ and $\tilde{h} = \sqrt{14\pi/M} \approx 0.147$. The settings of ζ_0 in (a) and (b) correspond to (3.8) and (3.9), respectively. The function μ and the parameters above are also adopted in Example 1 in Section 4. The approximate values (3.3) and their errors are computed for $\zeta = 0, \tilde{h}, \dots, N_\gamma \tilde{h}, \dots, M\tilde{h}$ with double precision and shown for $\zeta = 0, \tilde{h}, \dots, N_\gamma \tilde{h}, \dots, \lfloor M/1.5 \rfloor \tilde{h}$ in the graphs above. In case (a), the errors for $\zeta \in [0, 2\zeta_0]$ are small whereas they rapidly become large as ζ increases. In case (b), almost all errors for $\zeta \in [0, 2\zeta_0]$ are small except for some ζ near both sides of $[0, 2\zeta_0]$. Note that $N_\gamma \tilde{h} \approx 150$.

The *nonuniform FFT* (Dutt & Rokhlin, 1993, 1995; Greengard & Lee, 2004; Potts *et al.*, 2001; Steidl, 1998) is a fast method to compute the DFT in (3.10) with a nonuniform grid such as $\{y_j\}$ defined by (3.12). To use the technique of the nonuniform FFT, setting

$$\tilde{\Phi}[\mu]_j = \Phi[\mu]_j \exp(-i \lfloor N_\gamma/2 \rfloor \tilde{h} y_j), \quad (3.13)$$

$$k' = k - \lfloor N_\gamma/2 \rfloor, \quad (3.14)$$

we note the following relation:

$$\begin{aligned} \sqrt{\frac{\tau}{\pi}} e^{-\tau(ak')^2} \hat{\mu}_k &= \sum_{j=-M_-}^{M_+-1} \tilde{\Phi}[\mu]_j \sqrt{\frac{\tau}{\pi}} \exp(-\tau(ak')^2 - i(ak')(\tilde{h} y_j/a)) \\ &= \sum_{j=-M_-}^{M_+-1} \tilde{\Phi}[\mu]_j \frac{1}{2\pi} \int_{-\infty}^{\infty} \exp\left(-\frac{(v - \tilde{h} y_j/a)^2}{4\tau}\right) \exp(-iak'v) dv \\ &= \frac{1}{2\pi} \int_{-\infty}^{\infty} \left[\sum_{j=-M_-}^{M_+-1} \tilde{\Phi}[\mu]_j \exp\left(-\frac{(v - \tilde{h} y_j/a)^2}{4\tau}\right) \right] \exp(-iak'v) dv \\ &\approx \frac{\tilde{h}}{2\pi} \sum_{l=-L_-}^{L_+-1} \left[\sum_{j=-M_-}^{M_+-1} \tilde{\Phi}[\mu]_j \exp\left(-\frac{(l\tilde{h} - \tilde{h} y_j/a)^2}{4\tau}\right) \right] \exp(-ia\tilde{h}k'l), \end{aligned} \quad (3.15)$$

where τ , a , \check{h} , and L_{\pm} are positive constants to be determined appropriately. To decrease the computational cost of the sum in $[\]$ in (3.15), we neglect the sufficiently small summands present in it

$$\sum_{j=-M_-}^{M_+-1} \tilde{\Phi}[\mu]_j \exp\left(-\frac{(l\check{h}-\check{h}y_j/a)^2}{4\tau}\right) \approx \sum_{j \in J(l)} \tilde{\Phi}[\mu]_j \exp\left(-\frac{(l\check{h}-\check{h}y_j/a)^2}{4\tau}\right), \quad (3.16)$$

where $J(l)$ is the set of the indexes defined by

$$J(l) = \{j \mid |l\check{h}-\check{h}y_j/a| \leq b\} \quad (3.17)$$

for some $b > 0$. Since y_j is defined by φ in (3.1) as (3.12) and monotone increasing with respect to j , the index set $J(l)$ is contained in the slightly augmented set $\tilde{J}(l)$ defined by

$$\tilde{J}(l) = \{j \mid j_{\min}(l) \leq j \leq j_{\max}(l)\}, \quad (3.18)$$

where

$$j_{\min}(l) = \max\{j \mid l \geq \lceil (\check{h}y_j/a + b)/\check{h} \rceil\}, \quad (3.19)$$

$$j_{\max}(l) = \max\{j \mid l \geq \lfloor (\check{h}y_j/a - b)/\check{h} \rfloor\}. \quad (3.20)$$

Figure 2 shows examples of φ and $\tilde{J}(l)$. As explained in Remark 2 below, we can obtain $\tilde{J}(l)$ for $l = -L_-, \dots, L_+$ efficiently. The definition (3.18) of $\tilde{J}(l)$ means that the truncation error of approximation (3.16) is $O(\exp(-b^2/(4\tau)))$. Then, in addition to τ , a , \check{h} , and L_{\pm} , we need to choose the constant b so that both the total error (i.e., the sum of the discretization error for (3.15) and the truncation error for (3.16)) and the computational cost are reasonably small. For $M = M_- + M_+$ and a sufficiently small $\varepsilon > 0$ such as $\varepsilon = 10^{-10}$, we can present one possible set of their choices:¹

$$b = -\frac{2}{\pi} \log \varepsilon, \quad \tau = -\frac{1}{\pi^2} \log \varepsilon, \quad a = \frac{2\pi}{M}, \quad \check{h} = 1, \quad (3.21)$$

$$L_- = b - \left\lfloor \min_j (\check{h}y_j/a) \right\rfloor, \quad L_+ = -L_- + M - 1. \quad (3.22)$$

Under these settings, the total error of approximations (3.15) and (3.16) is approximately $O(\varepsilon)$. We may use larger b than the value above. Then, we can obtain the approximate values $\tilde{\mu}_k$ of $\hat{\mu}_k$ ($k = 0, \dots, N_\gamma$) as

$$\tilde{\mu}_k = \sqrt{\frac{\pi}{\tau}} e^{\tau(ak')^2} \frac{\check{h}}{2\pi} \sum_{l=-L_-}^{L_+} \left[\sum_{j \in \tilde{J}(l)} \tilde{\Phi}[\mu]_j \exp\left(-\frac{(l\check{h}-\check{h}y_j/a)^2}{4\tau}\right) \right] \exp\left(-i \frac{2\pi}{M} k'l\right), \quad (3.23)$$

where we can use the FFT for the outer sum. Under the settings of a and \check{h} in (3.21), the period of expression (3.23) with respect to k' is M . Therefore, we need to set

$$M_- + M_+ = M = 2N_\gamma \quad (3.24)$$

to compute the accurate approximations $\tilde{\mu}_k$ ($k = 0, \dots, N_\gamma$). Then, the computational cost is $O(bM) + O(M \log M) = O(N_\gamma \log N_\gamma)$.

¹When $\varepsilon = 10^{-10}$, $b = 14.65 \dots$ and $\tau = 2.33 \dots$ in (3.21).

Remark 1 In (3.15) and (3.23), we use the shifted index k' in (3.14) to avoid numerical instability in the actual computation of the approximate values $\tilde{\mu}_k$ in (3.23). In fact, if we use the factor $\sqrt{\pi/\tau}e^{\tau(ak)^2}$ in (3.23) as a usual manner of the nonuniform FFT, it becomes considerably large for a large k and the approximation gets worse.

Remark 2 The inequalities in (3.19) and (3.20) respectively defining j_{\min} and j_{\max} are nonlinear with respect to j , and it is difficult to obtain their closed forms. Therefore, noting the monotonicity of y_j with respect to j , we use the following numerical algorithms to determine them efficiently.

Algorithm for j_{\min}

```

begin
   $j_{\min}(-L_- - 1) = -M_-$ 
  for  $l = -L_-$  to  $L_+$ 
    for  $j = j_{\min}(l-1)$  to  $M_+ - 1$ 
      if  $l \geq \lceil (\tilde{h}y_j/a + b)/\tilde{h} \rceil$ 
         $j_{\min}(l) = j$ 
      else
        break
      end
    end
  end
end

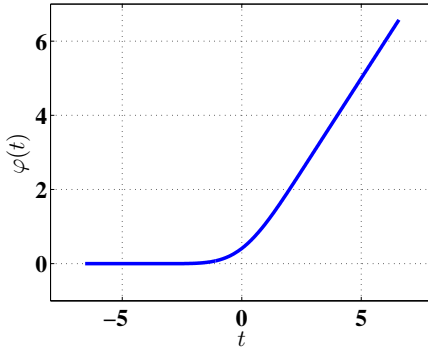
```

Algorithm for j_{\max}

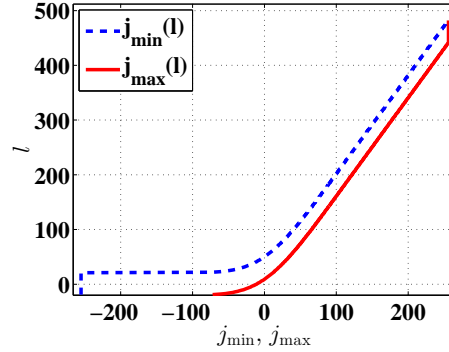
```

begin
   $j_{\max}(-L_- - 1) = -M_-$ 
  for  $l = -L_-$  to  $L_+$ 
    for  $j = j_{\max}(l-1)$  to  $M_+ - 1$ 
      if  $l \geq \lfloor (\tilde{h}y_j/a - b)/\tilde{h} \rfloor$ 
         $j_{\max}(l) = j$ 
      else
        break
      end
    end
  end
end

```



(a) Example of the function φ in (3.1).



(b) Example of the index set $\tilde{J}(l)$ in (3.18).

FIG. 2. Examples of φ in (3.1) and $\tilde{J}(l)$ in (3.18). (a) To fix φ , the following parameters are used: $M_- = M_+ = 2^8$, $M = M_- + M_+$, $N_\gamma = M/2$, $h = \log(10^3 M)/M \approx 0.026$, $\zeta_0 =$ (the value of (3.9)) ≈ 41.7 , $\beta = 0.25$, and $\alpha =$ (the value of (3.2)) ≈ 0.19 . (b) Functions j_{\min} and j_{\max} are defined by (3.19) and (3.20), respectively. To fix them, \tilde{h} is determined by $\tilde{h} = \sqrt{14\pi/M} \approx 0.29$, and a and \tilde{h} are determined by (3.21): $a = 2\pi/M \approx 0.012$, $\tilde{h} = 1$. Finally, $b = 20$. The parameters stated above are also adopted in Example 1 in Section 4.

3.2 Step 2: Computation of the indefinite integral of (2.9) in (2.5) or (2.7)

In this step, using the values $\tilde{\mu}_{-N_\gamma+1}, \dots, \tilde{\mu}_{N_\gamma}$, i.e., the approximate values of (2.9) for $\zeta = k\tilde{h}$ ($k = -N_\gamma + 1, \dots, N_\gamma$), we obtain the approximate values of the indefinite integral (2.9) in (2.5) or (2.7) for $\omega = \ell\tilde{h}$ ($\ell = -N + 1, \dots, N$). Recall that N is the integer determining the number of x 's for which we want to compute the values of the solution $p(x, t)$ in (2.8). Noting (3.7), we have only to compute the approximate values for $\omega = \ell\tilde{h}$ ($\ell = 1, \dots, N$).

3.2.1 Sinc-Gauss indefinite integration formula. Let N' be a positive integer. As a tool for computing indefinite integrals, we use the sinc-Gauss sampling formula (Tanaka *et al.*, 2008) for a function f on \mathbf{R}

$$f(\zeta) \approx \mathcal{T}_{N', \tilde{h}} f(\zeta) = \sum_{k=\lfloor \zeta/\tilde{h} \rfloor - N' + 1}^{\lfloor \zeta/\tilde{h} \rfloor + N'} f(k\tilde{h}) \operatorname{sinc}(\zeta/\tilde{h} - k) \exp\left(-\frac{(\zeta/\tilde{h} - k)^2}{2r^2}\right), \quad (3.25)$$

where $\operatorname{sinc}(\zeta) = \sin(\pi\zeta)/(\pi\zeta)$. The error estimate of this formula is given by the following theorem, which is a combination of the special cases of Lemmas 3.1 and 3.2 in Tanaka *et al.* (2008).

Theorem 1 ((Tanaka *et al.*, 2008, Lemmas 3.1, 3.2)) Let f be an analytic and bounded function in $\mathcal{D}_d = \{\zeta \in \mathbf{C} \mid |\operatorname{Im} \zeta| \leq d\}$ for some $d > 0$, and let $\mathcal{G}_{\tilde{h}} f(\zeta) = \lim_{N' \rightarrow \infty} \mathcal{T}_{N', \tilde{h}} f(\zeta)$. Then, for a sufficiently large N' and a sufficiently small $\tilde{h} > 0$, we have the following estimates of the discretization error (3.26) and the truncation error (3.27) of approximation (3.25):

$$\sup_{-\infty < t < \infty} |f(t) - \mathcal{G}_{\tilde{h}} f(t)| \leq Crh \exp\left(-\frac{\pi d}{\tilde{h}} + \frac{d^2}{2r^2\tilde{h}^2}\right), \quad (3.26)$$

$$\sup_{-\infty < t < \infty} \left| \mathcal{G}_{\tilde{h}} f(t) - \mathcal{T}_{N', \tilde{h}} f(t) \right| \leq C' \frac{r^2 e^{\frac{3}{2r^2}}}{N'^2} \exp\left(-\frac{N'^2}{2r^2}\right), \quad (3.27)$$

where C and C' are positive constants independent of N' , \tilde{h} , and r .

From formula (3.25), we derive a formula to approximate the indefinite integral of f from 0 to ω with $\omega = \ell\tilde{h}$ ($\ell = 1, \dots, N'$). Partitioning the integral of f as

$$\int_0^{\ell\tilde{h}} f(\zeta) d\zeta = \sum_{m=0}^{\ell-1} \int_{m\tilde{h}}^{(m+1)\tilde{h}} f(\zeta) d\zeta \quad (3.28)$$

and applying formula (3.25) to each term of the RHS in (3.28), we have

$$\begin{aligned} \int_0^{\ell\tilde{h}} f(\zeta) d\zeta &\approx \sum_{m=0}^{\ell-1} \sum_{k=m-N'+1}^{m+N'} f(k\tilde{h}) \int_{m\tilde{h}}^{(m+1)\tilde{h}} \operatorname{sinc}(\zeta/\tilde{h} - k) \exp\left(-\frac{(\zeta/\tilde{h} - k)^2}{2r^2}\right) d\zeta \\ &= \sum_{m=0}^{\ell-1} \sum_{k=m-N'+1}^{m+N'} f(k\tilde{h}) \tilde{h} (G_r(m+1-k) - G_r(m-k)), \end{aligned} \quad (3.29)$$

where

$$G_r(v) = \int_0^v \operatorname{sinc}(\eta) \exp\left(-\frac{\eta^2}{2r^2}\right) d\eta. \quad (3.30)$$

For $\ell = 1$, straightforwardly we have

$$\begin{aligned} (\text{RHS of (3.29)}) &= \sum_{k=-N'+1}^{N'} \tilde{h} f(k\tilde{h}) G_r(1-k) - \sum_{k=-N'+1}^{N'} \tilde{h} f(k\tilde{h}) G_r(-k) \\ &= \sum_{k'=-N'+1}^{N'} \tilde{h} f((1-k')\tilde{h}) G_r(k') - \sum_{k=-N'+1}^{N'} \tilde{h} f(k\tilde{h}) G_r(-k). \end{aligned} \quad (3.31)$$

For $\ell \geq 2$, setting $\tilde{f}_k = \tilde{h} f(k\tilde{h})$ and $d_a^b(G_r) = G_r(b) - G_r(a)$, we can rewrite the RHS of (3.29) as

$$(\text{RHS of (3.29)}) = \sum_{m=0}^{\ell-1} \sum_{k=m-N'+1}^{m+N'} \tilde{f}_k d_{m-k}^{m+1-k}(G_r) = \sum_{(m,k) \in I} \tilde{f}_k d_{m-k}^{m+1-k}(G_r), \quad (3.32)$$

where I is the set of indexes defined by

$$I = \bigcup_{m=0}^{\ell-1} \{(m, k) \mid m - N' + 1 \leq k \leq m + N'\}. \quad (3.33)$$

Here, we partition this index set I into three disjoint parts as

$$I = I_1 \cup I_2 \cup I_3, \quad (3.34)$$

where

$$I_1 = \bigcup_{k=N'+1}^{N'+\ell-1} \{(m, k) \mid k - N' \leq m \leq \ell - 1\}, \quad (3.35)$$

$$I_2 = \bigcup_{k=-N'+\ell}^{N'} \{(m, k) \mid 0 \leq m \leq \ell - 1\}, \quad (3.36)$$

$$I_3 = \bigcup_{k=-N'+1}^{-N'+\ell-1} \{(m, k) \mid 0 \leq m \leq k + N' - 1\}. \quad (3.37)$$

The type of this partition is illustrated by Figure 3. If we define S_i ($i = 1, 2, 3$) as

$$S_i = \sum_{(m,k) \in I_i} \tilde{f}_k d_{m-k}^{m+1-k}(G_r), \quad (3.38)$$

we have

$$(\text{RHS of (3.32)}) = S_1 + S_2 + S_3, \quad (3.39)$$

and

$$S_1 = \sum_{k=N'+1}^{N'+\ell-1} \sum_{m=k-N'}^{\ell-1} \tilde{f}_k d_{m-k}^{m+1-k}(G_r) = \sum_{k=N'+1}^{N'+\ell-1} \tilde{f}_k d_{-N'}^{\ell-k}(G_r), \quad (3.40)$$

$$S_2 = \sum_{k=-N'+\ell}^{N'} \sum_{m=0}^{\ell-1} \tilde{f}_k d_{m-k}^{m+1-k}(G_r) = \sum_{k=-N'+\ell}^{N'} \tilde{f}_k d_{-k}^{\ell-k}(G_r), \quad (3.41)$$

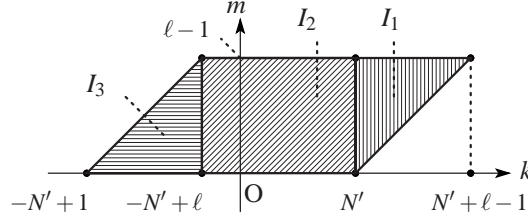


FIG. 3. Partition (3.34) of the index set I in (3.33). The index sets I_1 , I_2 , and I_3 consist of the integer lattice points in the corresponding regions above, respectively. The boundary between I_1 and I_2 , and the boundary between I_2 and I_3 belong to I_2 .

$$S_3 = \sum_{k=-N'+1}^{-N'+\ell-1} \sum_{m=0}^{k+N'-1} \tilde{f}_k d_{m-k}^{m+1-k}(G_r) = \sum_{k=-N'+1}^{-N'+\ell-1} \tilde{f}_k d_{-k}^{N'}(G_r). \quad (3.42)$$

Then, combining (3.32) and (3.39)–(3.42), we have

$$\begin{aligned} (\text{RHS of (3.29)}) &= \sum_{k=-N'+\ell}^{N'+\ell-1} \tilde{f}_k G_r(\ell-k) - \sum_{k=-N'+1}^{N'} \tilde{f}_k G_r(-k) \\ &\quad - G_r(-N') \sum_{k=N'+1}^{N'+\ell-1} \tilde{f}_k + G_r(N') \sum_{k=-N'+1}^{-N'+\ell-1} \tilde{f}_k. \end{aligned} \quad (3.43)$$

Letting $k' = \ell - k$, we can regard the first term of (3.43) as a discrete convolution

$$\sum_{k=-N'+\ell}^{N'+\ell-1} \tilde{h} f(k\tilde{h}) G_r(\ell-k) = \sum_{k'=-N'+1}^{N'} \tilde{h} f((\ell-k')\tilde{h}) G_r(k'). \quad (3.44)$$

Thus, rewriting k' as k in (3.31) and (3.44), we finally have an indefinite integration formula:

$$(\text{RHS of (3.29)}) = \sum_{k=-N'+1}^{N'} \tilde{h} f((\ell-k)\tilde{h}) G_r(k) - \sum_{k=-N'+1}^{N'} \tilde{h} f(k\tilde{h}) G_r(-k) + H_{\ell, N'}, \quad (3.45)$$

where

$$H_{\ell, N'} = \begin{cases} 0 & (\ell = 1), \\ -G_r(-N') \sum_{k=N'+1}^{N'+\ell-1} \tilde{h} f(k\tilde{h}) + G_r(N') \sum_{k=-N'+1}^{-N'+\ell-1} \tilde{h} f(k\tilde{h}) & (\ell = 2, \dots, N'). \end{cases} \quad (3.46)$$

To obtain the values of (3.45) for $\ell = 1, \dots, N'$, we need the $3N'$ values of $f(\zeta)$ for $\zeta = \ell\tilde{h}$ ($\ell = -N', \dots, 2N' - 1$).

Therefore, to compute the indefinite integral of (2.9) in (2.5) for $\omega = \ell\tilde{h}$ ($\ell = 1, \dots, N$), we set

$$N_1 = 2N \quad (3.47)$$

and use formula (3.45) with $N' = N$ and $f(\ell\tilde{h})$ replaced by $\tilde{\mu}_\ell$ for $\ell = -N, \dots, 2N - 1$. Furthermore, for the integral of (2.9) in (2.7), we set

$$N_2 = 4N \quad (3.48)$$

and use formula (3.45) twice with $N' = 2N$ for the first time and $N' = N$ for the second time.

In terms of computational time, note that the second term in (3.45) and $H_{\ell,N'}$ ($\ell = 2, \dots, N'$) in (3.46) can be computed in $O(N)$ time when $N' = N$ or $N' = 2N$. Then, what remains is to speed up the computation of the discrete convolution of the first term in (3.45). Extending the sum to a convolution with length $4N'$ and using the FFT as shown in Section 3.2.2 below, we can compute the discrete convolution of the first term in $O(N \log N)$ time when $N' = N$ or $N' = 2N$.

3.2.2 Fast computation of the convolution using the FFT. Consider the first term in (3.45) with $f((\ell - k)\tilde{h})$ replaced by $\tilde{\mu}_{\ell-k}$:

$$\tilde{h} \sum_{k=-N'+1}^{N'} \tilde{\mu}_{\ell-k} G_r(k). \quad (3.49)$$

We compute this convolution for $\ell = -N' + 1, \dots, N'$, although its values for $\ell = -N', \dots, 0$ are not required. To use the FFT for this computation, we define the sequence $\{g[r]_k\}_{k=-2N'+1}^{2N'}$ as

$$g[r]_k = \begin{cases} G_r(k) & (-N' + 1 \leq k \leq N'), \\ 0 & (-2N' + 1 \leq k \leq -N', N' + 1 \leq k \leq 2N'). \end{cases} \quad (3.50)$$

Then, we have

$$\tilde{h} \sum_{k=-N'+1}^{N'} \tilde{\mu}_{\ell-k} G_r(k) = \frac{\tilde{h}}{4N'} \sum_{m=-2N'+1}^{2N'} \text{DFT}[\tilde{\mu}]_m \text{DFT}[g[r]]_m e^{i \frac{2\pi}{4N'} \ell m} \quad (3.51)$$

for $\ell = -N' + 1, \dots, N'$, where

$$\text{DFT}[\tilde{\mu}]_m = \sum_{k_1=-2N'+1}^{2N'} \tilde{\mu}_{k_1} e^{-i \frac{2\pi}{4N'} k_1 m} \quad (m = -2N' + 1, \dots, 2N'), \quad (3.52)$$

$$\text{DFT}[g[r]]_m = \sum_{k_2=-2N'+1}^{2N'} g[r]_{k_2} e^{-i \frac{2\pi}{4N'} k_2 m} \quad (m = -2N' + 1, \dots, 2N'). \quad (3.53)$$

For the computation of (3.51), we need the values of $G_r(k)$ in (3.30). In fact, they can also be computed accurately by a Fourier-based method and the FFT as presented in Appendix A. Therefore, we can compute (3.51) by the FFT in $O(N \log N)$ time when $N' = N$ or $N' = 2N$.

Remark 3 Since the indefinite integration formula (3.45) is derived from the sinc-Gauss sampling formula (3.25), formula (3.45) inherits the error of formula (3.25) estimated in Theorem 1. In particular, the error of formula (3.45) is bounded by one of formula (3.25) multiplied by $N'\tilde{h}$. According to Theorem 1, the optimal settings of \tilde{h} and r for fixed N' are $\tilde{h} = d/N'$ and $r = \sqrt{N'/\pi}$, respectively, and the total error of formula (3.25) under these settings is $O(\sqrt{1/N'} \exp(-(\pi/2)N'))$ (Tanaka *et al.*, 2008,

Theorem 3.3). In this paper, however, we use the grid spacing \tilde{h} determined by (3.61) in Theorem 2 in Section 3.3 below, which results in $\tilde{h} = O(\sqrt{1/N'})$. This choice gives priority to the theoretical settings of the parameters in formula (3.56) for the inverse Fourier transform (2.8) in Step 3. Then, this \tilde{h} and $r = \sqrt{N'/\pi}$ yield the total error $O(\exp(-c\sqrt{N'}))$ of formula (3.25), which has a similar exponential part to error (3.62) of formula (3.56) with respect to N when $N' = N$ or $N' = 2N$.

Remark 4 The new formula (3.45) is introduced for fast computation of highly accurate approximations of an indefinite integral on the equispaced grid from the values of the integrand on the same grid. Among the traditional quadrature formulas, the Newton-Cotes formulas enable such computation. However, these formulas have errors $O(\tilde{h}^\kappa)$ for some $\kappa > 0$, and become algebraic with respect to N' when $\tilde{h} = O((N')^{-\lambda})$ for some $\lambda > 0$, whereas the formula (3.45) realizes the exponential convergence as shown in Remark 3.

Remark 5 The partition (3.34) of the index set I in (3.33) shown by Figure 3 is the key to the derivation of formula (3.45). A similar but different idea is proposed in Hale & Townsend (2014) for the computation of the convolution of functions.

3.3 Step 3: Computation of the inverse Fourier transform

Let $[\tilde{\mathcal{G}}_\gamma \mu]_N(\ell \tilde{h})$ ($\ell = -N+1, \dots, N$) denote the approximations of (2.5) or (2.7) computed in Step 2. In order to approximate the inverse Fourier transform (2.8), we use the formula for the Fourier transform with a continuous Euler transform introduced by Ooura (2001). Define $w(y; p, q)$ by

$$w(\xi; p, q) = \frac{1}{2} \operatorname{erfc} \left(\frac{\xi}{p} - q \right), \quad (3.54)$$

where erfc is the complementary error function defined as

$$\operatorname{erfc}(\xi) = \frac{2}{\sqrt{\pi}} \int_{\xi}^{\infty} \exp(-t^2) dt. \quad (3.55)$$

Using $w(\xi; p, q)$ as a weight function, we consider the following approximations of (2.8):

$$\begin{aligned} \frac{1}{2\pi} \int_{-\infty}^{\infty} \exp(t [\mathcal{G}_\gamma \mu](\omega)) e^{ix\omega} d\omega &\approx \frac{1}{2\pi} \int_{-\infty}^{\infty} w(|\omega|; p, q) \exp(t [\mathcal{G}_\gamma \mu](\omega)) e^{ix\omega} d\omega \\ &\approx \frac{\tilde{h}}{2\pi} \sum_{\ell=-N+1}^N w(|\ell \tilde{h}|; p, q) \exp(t [\tilde{\mathcal{G}}_\gamma \mu]_N(\ell \tilde{h})) e^{ix\ell \tilde{h}}. \end{aligned} \quad (3.56)$$

The formula (3.56) is the formula for the Fourier transform with a continuous Euler transform. The role of the function $w(|\omega|; p, q)$ is to realize the rapid decay of the integrand as $|\omega| \rightarrow \infty$ on \mathbf{R} . Then, we need to compute the values of (3.56) for $x = n\hat{h}$ ($n = -N+1, \dots, N$). Substituting this expression of x into the factor $e^{ix\ell \tilde{h}}$ in (3.56), we have

$$\exp(ix\ell \tilde{h}) = \exp(i\tilde{h}\hat{h}\ell n). \quad (3.57)$$

Unless the Nyquist condition $\tilde{h}\hat{h} = \pi/N$ holds, we cannot apply the FFT directly to the computation of (3.56). Therefore, for this computation, we use the fractional FFT (Bailey & Swartztrauber, 1991) that enables fast computation of the DFT without the Nyquist condition. Then, we can compute (3.56) in $O(N \log N)$ time. The details of the fractional FFT combined with the formula (3.56) is explained in Tanaka (2014a). The error bound of the formula (3.56) is given by Theorem 4 in Tanaka (2014a).

Theorem 2 ((Tanaka, 2014a, Theorem 4)) Let f be a function analytic and bounded in $\mathcal{T}'_\theta \cup \mathcal{D}_d$ for some θ with $0 < \theta < \pi/2$ and $d > 0$, where

$$\mathcal{T}'_\theta = \{z \in \mathbf{C} \mid |\arg z| < \theta \text{ or } |\pi - \arg z| < \theta\}, \quad (3.58)$$

$$\mathcal{D}_d = \{z \in \mathbf{C} \mid |\operatorname{Im} z| < d\}. \quad (3.59)$$

Moreover, assume that

$$\lim_{R \rightarrow \infty} \max_{-\theta \leq \phi \leq \theta} |f(\pm R + i(\tan \phi)R)| = 0 \quad (3.60)$$

and f is square integrable on \mathbf{R} . Let x_l and x_u be real numbers with $0 < x_l < x_u$ and $x_l/x_u \leq \min\{\tan \theta, 1/2\}$. Then, for any x with $x_l \leq |x| \leq x_u$ and a sufficiently large integer $N > 0$, defining h, p, q by

$$\tilde{h} = \sqrt{\frac{2\pi d(x_l + x_u)}{x_l^2 N}}, \quad p = \sqrt{\frac{N\tilde{h}}{x_l}}, \quad q = \sqrt{\frac{x_l N \tilde{h}}{4}}, \quad (3.61)$$

we have

$$\left| \int_{-\infty}^{\infty} f(\omega) e^{ix\omega} d\omega - \tilde{h} \sum_{\ell=-N+1}^N w(|\ell\tilde{h}|; p, q) f(\ell\tilde{h}) e^{ix\ell\tilde{h}} \right| = O \left[\sqrt{N} \exp \left(-\sqrt{\frac{\pi d x_l^2 N}{2(x_l + x_u)}} \right) \right]. \quad (3.62)$$

Remark 6 Since the assumption of Theorem 2 includes the case that f is not absolute integrable on \mathbf{R} , the Fourier transform of f may be discontinuous or non-smooth at the origin $x = 0$. Then, we consider the positive lower bound x_l of the absolute value of x to avoid the error estimate around the origin. See Tanaka (2014a) for the details of the error estimate.

Remark 7 We use the different formulas (3.3) and (3.56) for the Fourier transforms (2.9) and (2.8), respectively. This is because the former Fourier transform (2.9) is the integral on the semi-infinite interval $[0, \infty)$ whereas the latter Fourier transform (2.8) is one on the infinite interval $(-\infty, \infty)$. Further, we can also use formula (3.3) for (2.8) by partitioning the interval $(-\infty, \infty)$ to $(-\infty, 0]$ and $[0, \infty)$. However, we give priority to a brief implementation and lower computational cost of formula (3.56).

4. Numerical examples

In this section, we apply the proposed method to two examples of the PIDE (1.9) with initial condition $p(x, 0) = \delta(x)$. Let K_ν be the modified Bessel function of the second kind.

Example 1 (Variance gamma (VG) process (Applebaum, 2009)) Setting $\gamma = 1$ and $\mu(y) = e^{-y}$ in (1.8), we have the Lévy measure

$$\nu(dy) = \frac{1}{|y|} e^{-|y|} dy. \quad (4.1)$$

The Lévy process described by this measure is the symmetric VG process. The exact solution of (1.9) with measure (4.1) is written in the form

$$p(x, t) = \left(\frac{|x|}{2} \right)^{t-1/2} \frac{K_{1/2-t}(|x|)}{\sqrt{\pi} \Gamma(t)}. \quad (4.2)$$

Example 2 (Normal inverse Gaussian (NIG) process (Applebaum, 2009)) Setting $\gamma = 2$ and $\mu(y) = yK_1(y)/\pi$ in (1.8), we have the Lévy measure

$$\nu(dy) = \frac{1}{\pi|y|} K_1(|y|) dy. \quad (4.3)$$

The Lévy process described by this measure is the symmetric NIG process. The exact solution of (1.9) with measure (4.3) is written in the form

$$p(x, t) = t e^t \frac{K_1(\sqrt{x^2 + t^2})}{\pi \sqrt{x^2 + t^2}}. \quad (4.4)$$

Using the proposed method, we compute the numerical solutions of these examples for $x \in [-5, 5]$ and $t = 1, 2, 3$. Then, x_u in Theorem 2 should be set as $x_u = 5$. In addition, we choose $x_l = 2$. To set equispaced grids on $[-5, 5]$, we consider the sampling points $x = n\hat{h}$ ($n = -N + 1, \dots, N$) with $\hat{h} = 5/N$ for

$$N = 2^{i-i_\gamma} \quad (i = 7, \dots, 12), \quad (4.5)$$

where $i_1 = 2$ for Example 1 and $i_2 = 3$ for Example 2. The other parameters in the proposed method are determined as described below.

Step 1 For Example 1, $M = 4N$ and $N_1 = 2N$ according to (3.24) and (3.47). For Example 2, $M = 8N$ and $N_2 = 4N$ according to (3.24) and (3.48). In addition, $\tilde{h} = \sqrt{7\pi/(2N)}$ according to Theorem 2, where we use $d = 1$. The other parameters required in Step 1 are as follows:

$$M_- = M/2, \quad M_+ = M - M_-, \quad h = \log(10^3 M)/M, \quad (4.6)$$

$$\zeta_0 = [\text{the values of (3.8) and (3.9)}], \quad \beta = 0.25, \quad \alpha = [\text{the value of (3.2)}], \quad (4.7)$$

$$b = 20, \quad (\tau, a, \tilde{h}, L_\pm) = [\text{the set of the values of (3.21) and (3.22) for } \varepsilon = 10^{-10}]. \quad (4.8)$$

Step 2 According to Theorem 1 and Remark 3, we set $r = \sqrt{N'/\pi}$ in the Gaussian kernel in (3.30), where $N' = N$ for Example 1, and $N' = 2N$ and $N' = N$ in the first and second application of the indefinite integral formula, respectively, for Example 2.

Step 3 According to Theorem 2, we set $p = q = \sqrt{N\tilde{h}/2}$ because $x_l = 2$.

In (4.6), h is not set based on a theoretical criterion but it is determined experimentally in reference to the settings in the DE formulas for definite integration (Tanaka *et al.*, 2009). All computations are performed through MATLAB R2013a programs with double precision floating point arithmetic on a PC with a 3.0 GHz CPU and 2.0 GB RAM. The Matlab codes used for the computations are exposed on web page Tanaka (2014b).

Results of these numerical experiments are shown below. First, for reference, the exact solutions of (4.2) of Example 1 for $t = 1, 2, 3$ are displayed in Figure 4. The errors of Example 1 for $M = 2^{11}$ and $t = 1, 2, 3$ are plotted in Figure 5. The maximums of the errors of Example 1 on the intervals $[-x_u, x_u]$ and $[-x_u, -x_l] \cup [x_l, x_u]$ for every M 's are plotted for $t = 1, 2$, and 3 in Figures 6, 7, and 8, respectively. The errors on $[-x_u, x_u]$ are computed to observe the errors which are not estimated by Theorem 2. The computational times of Example 1 for only $t = 3$ are shown by Figure 9 because ones for $t = 1, 2$ are considerably similar. Next, the exact solutions of (4.4) of Example 2 for $t = 1, 2, 3$ are displayed in

Figure 10. The errors of Example 2 for $M = 2^{11}$ and $t = 1, 2, 3$ are plotted in Figure 11. The maximums of the errors of Example 2 on the intervals $[-x_u, x_u]$ and $[-x_u, -x_l] \cup [x_l, x_u]$ for every M 's are plotted for $t = 1, 2$, and 3 in Figures 12, 13, and 14, respectively. The computational times of Example 2 for only $t = 3$ are shown by Figure 15 because ones for $t = 1, 2$ are considerably similar.

The errors of Example 1 on the interval $[-x_u, -x_l] \cup [x_l, x_u]$ seems to have order $O(\exp(-c\sqrt{M}))$ for some $c > 0$ according to Figures 6–8. This observation, Theorems 1 and 2, and Remark 3 imply that the leading error occurs in Step 2 or 3 of the proposed method. On the other hand, in particular for $t = 1$, the errors of Example 1 on the interval $[-x_u, x_u]$ are worse than ones on $[-x_u, -x_l] \cup [x_l, x_u]$. We can guess that this phenomenon is due to the cusp of the solution (4.2) at the origin shown by Figure 4. In fact, as time t increases, the peakedness of the solution becomes gentler and the errors around the origin improve. In addition, the computational times shown by Figure 15 are approximately consistent with the theoretical estimate $O(N \log N) = O(M \log M)$. As for the results of Example 2, we can obtain similar observations for the errors on the interval $[-x_u, -x_l] \cup [x_l, x_u]$ and the computational times. However, the errors of Example 2 on the interval $[-x_u, x_u]$ are as good as the ones on $[-x_u, -x_l] \cup [x_l, x_u]$, which may be because solution (4.4) does not have sharp cusp for $t = 1, 2, 3$.

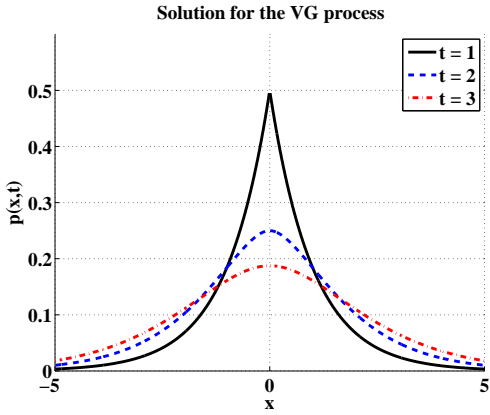


FIG. 4. Exact solutions $p(x, t)$ in (4.2) of Example 1

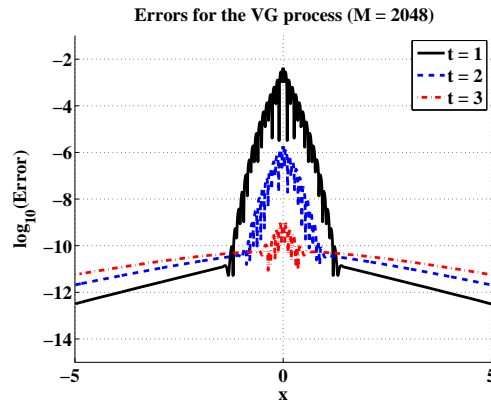


FIG. 5. Errors of the numerical solutions for Example 1 when $t = 1, 2, 3$ and $M = 2^{11}$ (i.e., $N = 2^9$)

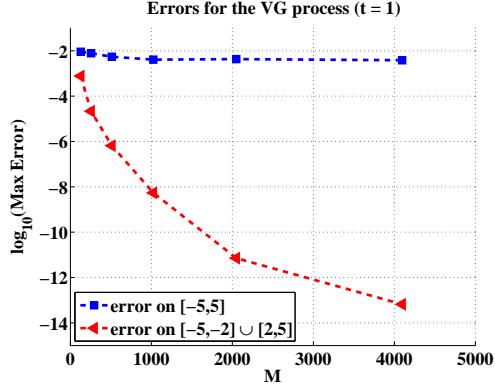


FIG. 6. Errors of the numerical solutions on $[-5,5]$ and $[-5,-2] \cup [2,5]$ for Example 1 when $t = 1$ and $M = 2^7, \dots, 2^{12}$ (i.e., $N = 2^5, \dots, 2^{10}$)

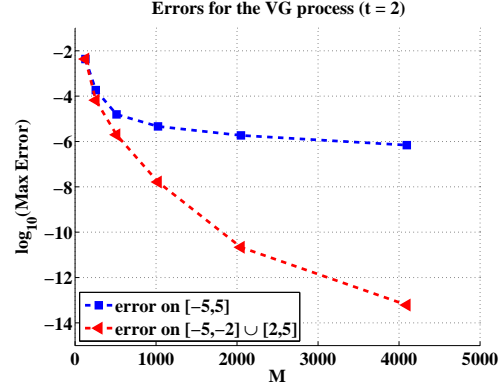


FIG. 7. Errors of the numerical solutions on $[-5,5]$ and $[-5,-2] \cup [2,5]$ for Example 1 when $t = 2$ and $M = 2^7, \dots, 2^{12}$ (i.e., $N = 2^5, \dots, 2^{10}$)

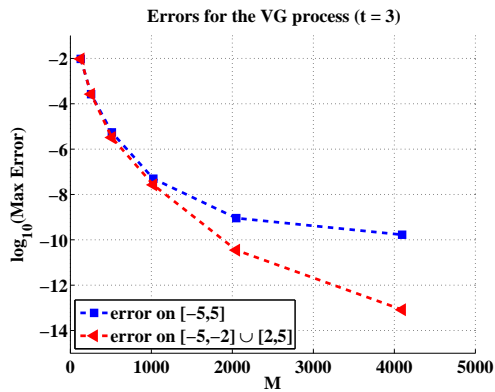


FIG. 8. Errors of the numerical solutions on $[-5,5]$ and $[-5,-2] \cup [2,5]$ for Example 1 when $t = 3$ and $M = 2^7, \dots, 2^{12}$ (i.e., $N = 2^5, \dots, 2^{10}$)

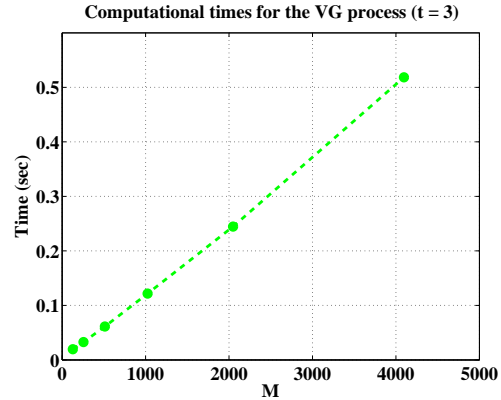
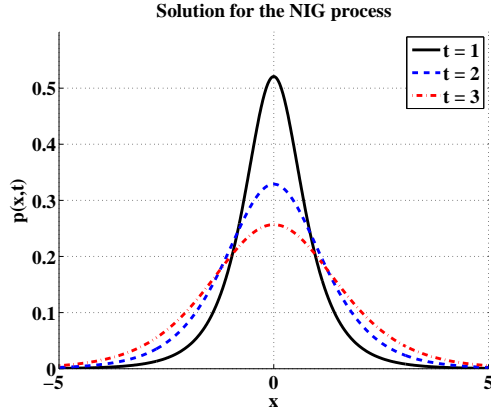
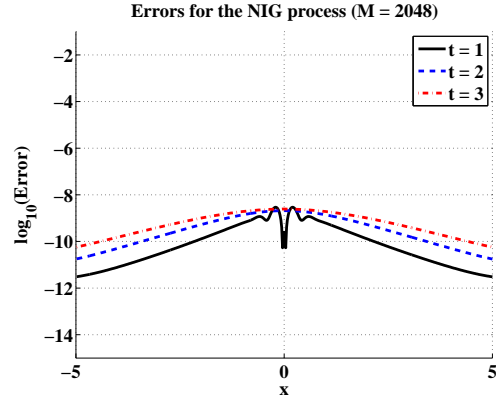
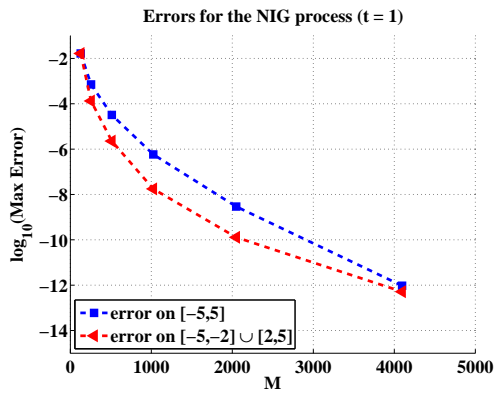
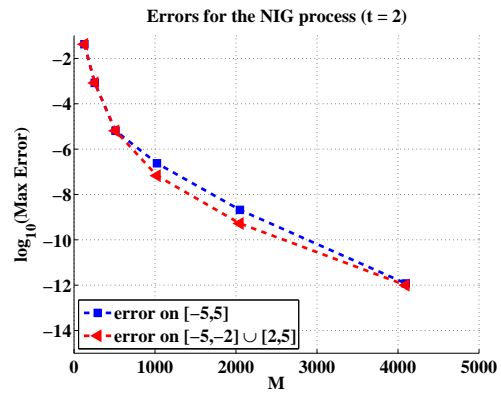


FIG. 9. Computational times for Example 1 when $t = 3$ and $M = 2^7, \dots, 2^{12}$ (i.e., $N = 2^5, \dots, 2^{10}$)

FIG. 10. Exact solutions $p(x,t)$ in (4.4) of Example 2FIG. 11. Errors of the numerical solutions for Example 2 when $t = 1, 2, 3$ and $M = 2^{11}$ (i.e., $N = 2^8$)FIG. 12. Errors of the numerical solutions on $[-5,5]$ and $[-5,-2] \cup [2,5]$ for Example 2 when $t = 1$ and $M = 2^7, \dots, 2^{12}$ (i.e., $N = 2^4, \dots, 2^9$)FIG. 13. Errors of the numerical solutions on $[-5,5]$ and $[-5,-2] \cup [2,5]$ for Example 2 when $t = 2$ and $M = 2^7, \dots, 2^{12}$ (i.e., $N = 2^4, \dots, 2^9$)

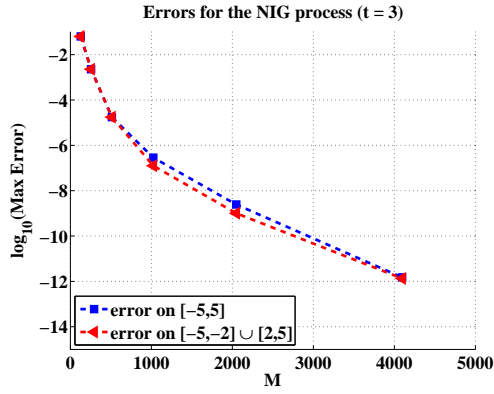


FIG. 14. Errors of the numerical solutions on $[-5, 5]$ and $[-5, -2] \cup [2, 5]$ for Example 2 when $t = 3$ and $M = 2^7, \dots, 2^{12}$ (i.e., $N = 2^4, \dots, 2^9$)

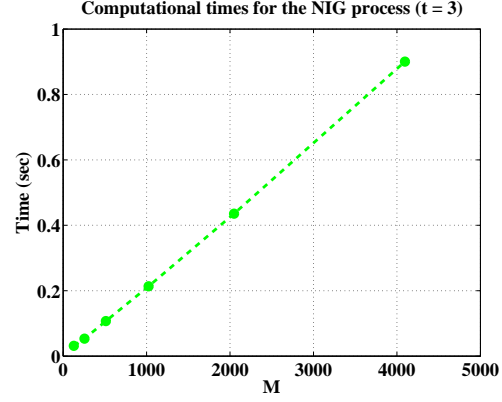


FIG. 15. Computational times for Example 1 when $t = 3$ and $M = 2^7, \dots, 2^{12}$ (i.e., $N = 2^4, \dots, 2^9$)

5. Concluding remarks

In this paper, we proposed a fast and accurate numerical method to solve the Kolmogorov forward equations (1.9) of the scalar Lévy processes with symmetric measures (1.8). The method consists of the three steps presented in Sections 2 and 3. Step 1 and 3 are respectively based on accurate numerical formulas (3.3) and (3.56) for the Fourier transform proposed by Ooura (2001, 2005), which are respectively combined with the nonuniform FFT and the fractional FFT to speed up the computations. Step 2 requires numerical indefinite integration on the equispaced grids. This computation is performed using formula (3.45) obtained by integrating the sinc-Gauss sampling formula (3.25) and combining the resultant convolution in (3.45) with the FFT. The numerical solutions by the proposed method seemed to be exponentially convergent on the interval without sharp cusps of the corresponding exact solutions. Furthermore, the real computational times were approximately consistent with the theoretical estimate $O(N \log N)$, where N is the half of the number of the points x on which the approximations of the solutions $p(x, t)$ were computed for a fixed t . As subjects of future works, we can consider the followings: the rigorous theoretical estimate of the errors of the proposed method, the optimal determination of the parameters based on the estimate, the comparison of the proposed method with other similar methods, and the extension of the method to broader class of Lévy processes.

Acknowledgments

The author would like to thank Prof. L. N. Trefethen for his valuable comments regarding the sinc-Gauss indefinite integration formula in Step 2 of the proposed method in a private seminar at the University of Tokyo in March 2014. He also informed the author about reference Hale & Townsend (2014). This work is supported by JSPS KAKENHI Grant Number 24760064.

REFERENCES

APPLEBAUM, D. (2009) *Lévy Processes and Stochastic Calculus*, 2nd edn. Cambridge: Cambridge University Press.

- BAILEY, D. H. & SWARZTRAUBER, P. N. (1991) The fractional Fourier transform and applications. *SIAM Rev.*, **33**, 389–404.
- BUENO-OROVIO, A., KAY, D. & BURRAGE, K. (2014) Fourier spectral methods for fractional-in-space reaction-diffusion equations. *BIT Numer. Math.*, DOI 10.1007/s10543-014-0484-2.
- CARR, P. & MADAN, D. B. (1999) Option valuation using the fast Fourier transform. *J. Comput. Finance*, **2**, 61–73.
- CHOURDAKIS, K. (2005) Option pricing using the fractional FFT. *J. Comput. Finance*, **8**, 1–18.
- CONT, R. & VOLTCHKOVA, E. (2005) Integro-differential equations for option prices in exponential Levy models. *Finance Stochast.*, **9**, 299–325.
- DUQUESNE, T., REICHMANN, O., SATO, K. & SCHWAB, C. (2010) *Lévy Matters I: Recent Progress in Theory and Applications: Foundations, Trees and Numerical Issues in Finance*. Lecture Notes in Mathematics, vol. 2001. Heidelberg: Springer.
- DUTT, A. & ROKHLIN, V. (1993) Fast Fourier transforms for nonequispaced data. *SIAM J. Sci. Comput.*, **14**, 1368–1393.
- DUTT, A. & ROKHLIN, V. (1995) Fast Fourier transforms for nonequispaced data II. *Appl. Comput. Harmon. Anal.*, **2**, 85–100.
- FANG, F & OOSTERLEE, C. W. (2008) A novel pricing method for European options based on Fourier-cosine series expansions. *SIAM J. Sci. Comput.*, **31**, 826–848.
- GAO, T., DUAN, J. & LI, X. (2013) Fokker-Planck equations for stochastic dynamical systems with symmetric Lévy motions. arXiv:1310.7677.
- GARDINER, C. (2009) *Stochastic Methods: A Handbook for the Natural and Social Sciences*, 4th edn. Heidelberg: Springer.
- GARREAU, P. & KOPRIVA, D. (2013) A spectral element framework for option pricing under general exponential Lévy processes. *J. Sci. Comput.*, **57**, 390–413.
- GREENGARD, L. & LEE, J. Y. (2004) Accelerating the nonuniform fast Fourier transform. *SIAM Rev.*, **46**, 443–454.
- HALE, N. & TOWNSEND, A. (2014) An algorithm for the convolution of Legendre series. *SIAM J. Sci. Comput.*, **36**, A1207–A1220.
- HUANG, J., NIE, N. & TANG, Y. (2014) A second order finite difference-spectral method for space fractional diffusion equations. *Sci. China Math.*, **57**, 1303–1317.
- HUANG, Y. & OBERMAN, A. (2013) Numerical methods for the fractional Laplacian Part I: a finite difference-quadrature approach. arXiv:1311.7691.
- KOZUBOWSKI, T. J., MEERSCHAERT, M. M. & PODGÓRSKI, K. (2006) Fractional Laplace motion, *Adv. Appl. Prob.*, **38**, 451–464.
- KWOK, Y. K., LEUNG, K. S. & WONG, H. Y. (2012) Efficient options pricing using the fast Fourier transform. *Handbook of Computational Finance* (J.-C. Duan *et al.* eds). Berlin: Springer, pp. 579–604.
- LEE, S. T., LIU, X. & SUN, H.-W. (2012) Fast exponential time integration scheme for option pricing with jumps. *Numer. Linear Algebra Appl.*, **19**, 87–101.
- LI, C., DENG, W. & WU, Y. (2012) Finite difference approximations and dynamics simulations for the Levy fractional Klein-Kramers equation. *Numer. Methods Partial Differential Equations*, **28**, 1944–1965.
- LENZI, E. K., MENDES, R. S., KWOK, S. F. & MALACARNE, L. C. (2003) Anomalous diffusion: fractional Fokker-Planck equation and its solutions. *J. Math. Phys.*, **44**, 2179–2185.
- MEERSCHAERT, M. M. & TADJERAN, C. (2004) Finite difference approximations for fractional advection-dispersion flow equations. *J. Comput. Appl. Math.*, **172**, 65–77.
- OOURA, T. (2001) A continuous Euler transformation and its application to Fourier transform of a slowly decaying function. *J. Comput. Appl. Math.*, **130**, 259–270.
- OOURA, T. (2005) A double exponential formula for the Fourier transforms. *Publ. RIMS Kyoto Univ.*, **41**, 971–977.
- POTTS, D., STEIDL, G. & TASCHKE, M. (2001) Fast Fourier transforms for nonequispaced data: A tutorial. *Modern*

- Sampling Theory: Mathematics and Applications.* (J. J. Benedetto & P. Ferreira, eds). Boston: Birkhäuser, pp. 249–274.
- SABATIER, J., AGRAWAL, O. P. & TENREIRO MACHADO, J. A. (2007) *Advances in Fractional Calculus: Theoretical Developments and Applications in Physics and Engineering.* Springer.
- STEIDL, G. (1998) A note on fast Fourier transforms for nonequispaced grids. *Adv. Comput. Math.*, **9**, 337–352.
- TANAKA, K. (2014a) Error control of a numerical formula for the Fourier transform by Ooura’s continuous Euler transform and fractional FFT. *J. Comput. Appl. Math.*, **266**, 73–86.
- TANAKA, K. (2014b) Matlab codes for the symmetric Levy processes.
https://github.com/KeTanakaN/mat_symLevy_FT_codes (accessed 1 August 2014).
- TANAKA, K., SUGIHARA, M. & MUROTA, K. (2008) Complex-analytic approach to the sinc-Gauss sampling formula. *Japan J. Indust. Appl. Math.*, **25**, 209–231.
- TANAKA, K., SUGIHARA, M., MUROTA, K. & MORI, M. (2009) Function classes for double exponential integration formulas. *Numer. Math.*, **111**, 631–655.
- YAN, L. (2013) Numerical solutions of fractional Fokker-Planck equations using iterative Laplace transform method. *Abstr. Appl. Anal.*, **2013**, Art. ID 465160.
- ZHAO, Z. & LIB, C. (2012) A numerical approach to the generalized nonlinear fractional Fokker-Planck equation. *Comput. Math. Appl.*, **64**, 3075–3089.

Appendix A. Computation of the integrals of the sinc-Gauss kernel

In this section, we propose an efficient method to compute the values of $G_r(k)$ in (3.30), the integrals of the sinc-Gauss kernel. Let $F_{\text{SG}}(\omega)$ be the Fourier transform of the sinc-Gauss kernel

$$F_{\text{SG}}(\omega) = \int_{-\infty}^{\infty} \left[\text{sinc}(x) \exp\left(-\frac{x^2}{2r^2}\right) \right] \exp(-i\omega x) dx. \quad (\text{A.1})$$

Then, the function $F_{\text{SG}}(\omega)$ is written in the form

$$F_{\text{SG}}(\omega) = \frac{1}{2} \left[\text{erf}\left(\frac{r(\omega + \pi)}{\sqrt{2}}\right) - \text{erf}\left(\frac{r(\omega - \pi)}{\sqrt{2}}\right) \right], \quad (\text{A.2})$$

where erf is the error function defined as

$$\text{erf}(\xi) = \frac{2}{\sqrt{\pi}} \int_{-\infty}^{\xi} \exp(-t^2) dt. \quad (\text{A.3})$$

Using the function $F_{\text{SG}}(\omega)$ in (A.2), we have

$$\begin{aligned} G_r(k+1) - G_r(k) &= \int_k^{k+1} \left(\frac{1}{2\pi} \int_{-\infty}^{\infty} F_{\text{SG}}(\omega) \exp(ix\omega) d\omega \right) dx \\ &= \frac{1}{2\pi} \int_{-\infty}^{\infty} F_{\text{SG}}(\omega) \left(\int_k^{k+1} \exp(ix\omega) dx \right) d\omega \\ &= \frac{1}{2\pi} \int_{-\infty}^{\infty} F_{\text{SG}}(\omega) \text{sinc}(\omega/(2\pi)) \exp(i\omega/2) \exp(ik\omega) d\omega, \end{aligned} \quad (\text{A.4})$$

which is the inverse Fourier transform of the function $F_{\text{SG}}(\omega) \text{sinc}(\omega/(2\pi)) \exp(i\omega/2)$. Since the function $F_{\text{SG}}(\omega)$ rapidly decays as $|\omega| \rightarrow \infty$ on \mathbf{R} , applying the mid-point rule to integral (A.4), we can accurately approximate its values as

$$G_r(k+1) - G_r(k) \approx \frac{h'}{2\pi} \sum_{l'=-M+1}^M F_{\text{SG}}(l'h') \text{sinc}(l'h'/(2\pi)) \exp(il'h'/2) \exp(ikl'h'), \quad (\text{A.5})$$

24 of 24

where $h' = 2\pi/M$. This approximation is based on a similar principle as that of formula (3.56). Then, applying the fractional FFT to (A.5), we can obtain the approximate values of $G_r(k+1) - G_r(k)$ for $k = 0, 1, \dots, \lfloor M/2 \rfloor$ in $O(M \log M)$ time. Finally, adding them sequentially from $k = 0$ to $k = \lfloor M/2 \rfloor$, we can compute the approximations of $G_r(k)$ for $k = 0, 1, \dots, \lfloor M/2 \rfloor + 1$ in $O(M)$ time.